ACS APPLIED MATERIALS & INTERFACES

Research Article

www.acsami.org

Erosion Mechanism of MoS_2-Based Films Exposed to Atomic Oxygen Environments

Peng Wang,*[,†] Li Qiao,[†] Jiao Xu,[†] Wuxia Li,[‡] and Weimin Liu[†]

[†]State Key Laboratory of Solid Lubrication, Lanzhou Institute of Chemical Physics, Chinese Academy of Sciences, Lanzhou 730000, P.R. China

[‡]Beijing National Laboratory for Condensed Matter Physics, Institute of Physics, Chinese Academy of Sciences, Beijing 100190, China

ABSTRACT: The erosion mechanism of magnetron sputtered MoS_2 films exposed to the atomic oxygen environment was studied and compared with the Ti-doped MoS_2 and MoS_2/Ti multilayer films. The compositional and structural changes were investigated as a function of incident fluence by Rutherford back scattering (RBS) and focused ion beam combining with scanning electron microscopy (FIB&SEM). The RBS results indicate that the sulfur atoms are eroded by the incident atomic oxygen atoms and the removed sulfur amount increases but the erosion rate decreases with increasing of incident fluence. For pure MoS_2 films the erosion process turns to saturate at the end of investigated fluence of 4.8×10^{21} O cm^{-2}, and for Ti-doped and MoS_2/Ti multilayer films the saturation of sulfur erosion is much earlier around incident fluence of 5.2×10^{19} and 2.6×10^{19} O cm^{-2}, respectively. FIB cross-section results reveal that pores structures present in the as-deposited MoS_2 films provide a reaction highway, which allows the incident atomic oxygen to be able to reach and react with the sulfur at bottom. Introducing titanium doping or MoS_2/Ti multilayer structures definitely reduce the density of pores and defects in the initial films, consequently, erosion process is suppressed or blocked, and the instinct lubricant properties of MoS_2 phases can be well-retained in vacuum sliding conditions.

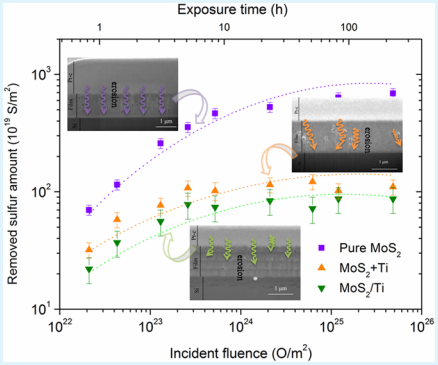

KEYWORDS: *atomic oxygen, exposure, MoS_2 films, erosion mechanism, titanium doping, multilayer*

1. INTRODUCTION

At the low earth orbit altitudes, the most abundant species is atomic oxygen, which is produced by dissociation of molecular oxygen under UV sunlight. Although the number density of this atomic oxygen is low, spacecraft move through it at high velocities. This results in high fluxes of atoms being swept onto the forward facing surface, with an effective translational energy of 5 eV. This energy value is high enough to break chemical bonds of most of the materials commonly used in space applications.[1−4] The reaction of materials with atomic oxygen in low earth orbit presents a safety concern on spacecraft operation. Consequently, much attention has been paid to the reaction between the energetic atomic oxygen and materials used in the exterior of a spacecraft, such as polymer and solid lubricants.[5−14]

Transition metal dichalcogenide such as MoS_2 have been widely used as solid lubricant films in aerospace applications because of their ultralow friction in ultrahigh vacuum or in inert gas environment. To improve the mechanical and tribological properties of these films, researchers have explored metal and ceramic incorporated as well as multilayer structures.[15−17] To evaluate the influence of atomic oxygen erosion on the properties of MoS_2 films, researchers have investigated the structure and property changes of these films due to atomic oxygen exposure both on laboratory simulation conditions and real spacecraft on low earth orbit. The previous research claimed that after atomic oxygen exposure the oxidation of MoS_2 films was restricted at surface within 3 nm region, the corresponding friction experiments reveal that although the initial friction coefficient increased but it recovered when the surface oxidation layer was removed by sliding.[2,12,13] For most of work, X-ray photoelectric spectroscopy (XPS) is used to investigate the composition changes of the films before and after atomic oxygen exposure because it is sensitive to evaluate the chemical bonding, but the quantitative results, such as the reaction amount of sulfur atoms with incident atomic oxygen cannot be obtained by XPS analysis. Furthermore, the total incident atomic oxygen fluence in these experiments is in the range of 1×10^{19} to 1×10^{21} atom cm^{-2}, which is much less compared to the integration incident fluence of spacecraft during long service life in low earth orbit. In addition, the most publications focus on comparing the structural and properties changes of the film before and after atomic oxygen exposure, but more details including the changes process, the influence of doped elements, and the effect of nanocomposite and multilayer structure are still unknown.

In this work, pure MoS_2, titanium-doped, and MoS_2/Ti multilayer films deposited by magnetron sputtering were used

Received: March 28, 2015
Accepted: May 27, 2015
Published: May 27, 2015

DOI: 10.1021/acsami.5b02709
ACS Appl. Mater. Interfaces 2015, 7, 12943−12950

to study the influence of atomic oxygen exposure on the compositional and structural changes. All erosion experiments were performed on a laboratory atomic oxygen beam with a flux of 7×10^{15} oxygen cm^{-2} s^{-1}. The compositional changes due to atomic oxygen exposure were quantitatively evaluated by Rutherford backscattering spectrometry, and the structural evolution was investigated using focused ion beam combining with scanning electron microscopy. More details were emphasized on the influence of introducing doping and multilayer structure on the erosion behavior. Furthermore, the impact of structure changes due to atomic oxygen erosion on tribological properties were investigated.

2. EXPERIMENTAL DETAILS

2.1. Film Deposition. The MoS_2, Ti-doped MoS_2, and MoS_2/Ti multilayer films were prepared on single-crystalline (100) silicon wafer using a commercial sputtering device. This device comprises 3 independently controllable magnetron sputter sources. For the experiments reported here, two of these sources were applied, one holding a MoS_2 target and the other a titanium target. The system was pumped down to a base pressure of less than 2×10^{-4} Pa and the deposition was performed in argon atmosphere. Prior to deposition, the silicon substrates were etched by argon plasma using a bias voltage of −600 V for 5 min to remove the natural oxide layer. Pure MoS_2 film was deposited with 275 W rf power at a working pressure of 7.5×10^{-1} Pa. Ti-doped MoS_2 film was deposited by applied 275 W rf power and 120 W dc power simultaneously to MoS_2 and titanium targets, respectively. The preparation process of the MoS_2/Ti multilayer structure was performed as following: at first, a 20 nm thick titanium layer was deposited on the silicon substrate, then about 300 nm thick MoS_2 was deposited on titanium layer, this deposition process was repeated four times and finally MoS_2/Ti multilayer structure was produced, in which four 300 nm thick MoS_2 films were separated by four 20 nm thick titanium layers, for each MoS_2 and Ti layer deposition 275 W rf power and 150 W dc power were applied to MoS_2 and titanium targets, respectively, and in both cases, the same working pressure about 7.5×10^{-1} Pa were used.

2.2. Atomic Oxygen Exposure. The atomic oxygen exposure experiments up to a fluence of 5×10^{21} O·cm^{-2} were performed on a laboratory simulation device. The MoS_2, Ti-doped MoS_2 and MoS_2/Ti multilayer films were exposed simultaneously to the atomic oxygen beam with defined fluence and for each exposure batch fresh deposited films were installed on sample holder. A basic description is given in.[9−11] In short, a microwaves (2.45 GHz) power source are coupled with a remote electron cyclotron resonance to produce plasma, once plasma was formed, it would become a beam under the effect of an electromagnetic field, and then be accelerated toward a molybdenum plate applied with a negative bias. The incident positive oxygen ions collides with the molybdenum plate and rebounded to form a neutral atomic oxygen beam with an impingement kinetic energy of 5 eV, which is as similar as the impact energy of atomic oxygen to material surface in low earth orbit. To ensure identical conditions in all exposure processes, the microwave output power was set to 200 W with a constant O_2 gas pressure prior to plasma ignition of 0.3 Pa (gas flow 30 sccm).

The flux of incident atomic oxygen beam was calibrated by measuring the mass loss of Kapton foil before and after exposure using the following formula

$$f = \frac{M}{g\delta st}$$

Where f is the erosion rate of Kapton foil, M is the mass loss of Kapton foil after certain time exposure, g corresponds to the density of Kapton, s and t represent the area and the time of Kapton foil exposed to atomic oxygen beam, δ is the erosion rate of Kapton, which is used as a constant value of 3.0×10^{-24} cm^3/atom in our experiment. The incident atomic oxygen flux according to the above calibration procedure was $7.2 \pm 0.2 \times 10^{15}$ O cm^{-2} s^{-1}. Because of the configuration of our device the present of negative oxygen ions in atomic beam is inevitably. To calibrate the ion flux of oxygen in impinging beam, tungsten films with a thickness of 300 nm deposited on silicon substrates was used as reference. A −200 V bias was applied on tungsten film during atomic oxygen exposure and the removed tungsten amount was measured by ion beam analysis. From the known sputtering yield (0.0193) of tungsten by oxygen,[18] the absolute ion flux can be determined by measuring the removed tungsten atom amount during defined sputtering times. After 48 h incident beam exposure (at −200 V bias) the total removal tungsten amount determined by RBS is 1.5×10^{17} W cm^{-2} (about 24 nm), corresponding to an ion flux about 4.5×10^{13} O cm^{-2} s^{-1}, which is 2 orders of magnitude lower compare to the flux of atomic oxygen.

2.3. Composition, Structure, and Tribological Properties Characterization. Rutherford Backscattering Spectrometry (RBS) was applied to measure the depth-resolved stoichiometry of the samples using a tandem accelerator at Max-Planck-Institut für Plasmaphysik, Garching. A beam of 3.0 MeV ^{4}He was used at a scattering angle of 165°, and a charge of 10 μC was usually accumulated for one RBS spectrum. The spectra were simulated using the program SIMNRA 6.05.[19] In order to detect morphological changes the cross sections of the films before and after exposure were imaged with scanning electron microscopy (SEM) combining with Focused Ion Beam (FIB). The used microscope (Helios NanoLab 600, FEI) allows the cross-sectioning in situ by the implemented 30 keV singly charged Ga^+ focused ion beam. The secondary electrons produced by a 5 keV electron beam were detected by the inlens detector system. The cross sections were imaged with the e-beam tilted by 38° to their surface plane, so that the vertical scale in the shown images is compressed relative to the horizontal scale. Before the cross-sectioning by FIB, first, a Pt composite strip that about 8.0 μm in length, 1.0 μm in width and 1.0 μm in thickness was deposited with an ion beam current of 80 pA as the mask for protection of the area of interest during focused-ion-beam milling. Then a rectangular pattern, 8 μm long and 6 μm wide was placed along the Pt strip and 2.5 nA ion beam current was used to etch the pattern about 2 μm deep into the substrate, which was followed by low ion beam current (≤40 pA) cleaning. The in situ scanning electron microscopy imaging was performed with accelerating voltage of 5 kV under beam current of 86 pA. The side-view was examined with the electron beam incident glancing angle of 52 degrees.

Tribological tests were performed by using a ball-on-disk tribometer on a low-pressure vacuum of 0.08 Pa at room temperature, and the relative humidity in testing chamber after pumping was about 20 ± 5%. AISI 400C steel ball with a diameter of 4 mm were used as counterpart. The friction experiments were performed in vacuum with a normal load of 3 N, a wear track in radius of 3 mm and disk rotational speed of 1000 rad/min (i.e., ball sliding velocity of 0.52 m/s) to a maximum sliding time of 60 min. After the friction test, dual mode 3D surface profilometer (AEP, USA) was applied to analyses the morphology of the wear tracks.

3. RESULTS AND DISCUSSION

3.1. Optimization Deposition Parameters. In the experiments, several tens of MoS_2 samples were used to expose to the atomic oxygen beam with different fluence, and the total areal density of each exposed MoS_2 film was measured by RBS to compare the composition changes as a function of incident fluence. Although all these samples deposited in the same batch, the difference of the distance from the target to samples may induce the inhomogeneous on the deposited films, which would lead to the difference on the initial areal density of each deposited film. Clearly, the present of difference on initial areal density in these model samples definitely reduces the accuracy of measurements and influences the data evaluation. To minimize the influence of the inhomogeneous of deposited MoS_2 films on the accuracy of the total areal density measurements, MoS_2 films were deposited in two independent

DOI: 10.1021/acsami.5b02709
ACS Appl. Mater. Interfaces 2015, 7, 12943−12950

batches to optimize the deposition parameters. In the first batch, 5 samples were fixed on the sample holder locating from the center to the edge with 20 mm interval that means during deposition the sample in the center is stationary and the other 4 samples rotate with the diameters of 20, 40, 60, and 80 mm, respectively. In the second deposition batch, except for the center position, 4 samples were placed on the position as same as first batch, but each sample shifts 45 deg along its original circle. After deposition, the total areal density was determined by RBS and the measured RBS spectra were quantitatively evaluated using the program SIMNRA.[19]

Figure 1 shows the typical 3 MeV ^{4}He RBS spectrum of MoS_2 film, in which the backscattering counts are plotted as a function of corresponding backscattering energy, the channel is shown on the top axis of the figure. Each peak and its height in these RBS spectra correspond to a certain element and its concentration. The width of the peak contains information on the film thickness and the intensity is correlated to the local concentration in a certain depth.[20] Several peaks were detected in RBS spectrum of Figure 1. They correspond to molybdenum, sulfur, and silicon. The surface position of each element and the corresponding positions of the interface for the as-deposited film are marked by the vertical dashed lines in Figure 1. For example, the high-energy edge of the Mo peak originates from Mo atoms at the surface and is marked as $Mo_{surface}$. The low-energy edge is accordingly due to Mo at the interface to the silicon substrate and is marked as $Mo_{interface}$.

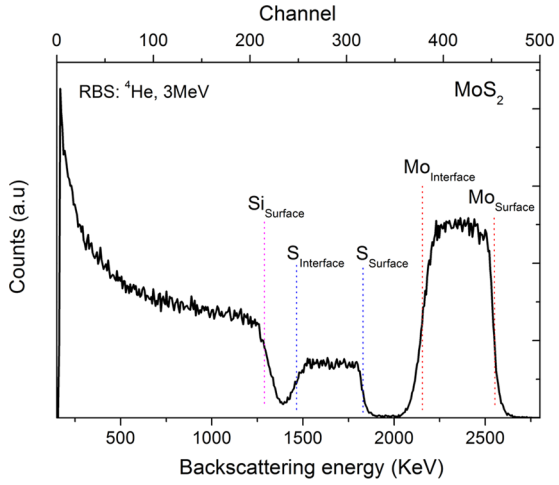

Figure 1. RBS spectrum of as-deposited MoS_2 films, the backscattering counts are plotted as a function of backscattering energy, and the corresponding channel is shown on the top axis of the figure. The backscattering energies for different atoms at the surface and at the interface to the substrate are marked by dotted lines for Mo, S, and Si.

The total Mo and S amount of the films deposited at different positions and batches are summarized in Figure 2. For all these samples the ratio between the S and Mo varies from 1.87 to 1.92, indicating a small amount of S atoms lost during sputtering deposition process. It can be seen that the total amount of Mo and S increase with the position of sample holder from the center to edge, resulting from the configuration of our deposition device, in which the target does not focus on the center of the sample holder, which leads to the inhomogeneous distribution of incident flux on. The total areal density of deposited MoS_2 film increases about 20% from the center to the edge. For the second deposition batch, the sample placed as the same position as the first deposition batch (at the center of the sample holder) shows only 2% variation on areal density of Mo and S atoms amount, and for other four samples deposited at the second batch the variation of total areal density fluctuates in 5%. Although in the second deposition batch the identical positions are different compare to the first batch because samples shift 45 deg along its original rotated circle, but each sample keeps the same rotated diameter because of the rotation of the sample holder, which contributes to the high repetition on the total areal density of deposited films. According to the above experimental results, it can be conclude that the total areal density of a serial of MoS_2 films within 5% variation can be obtained in one deposition batch if the samples placed on the sample holder with the same rotation diameter. In the following experiments, all MoS_2 films used to study the compositional changes were deposited in one batch, consequently, we ensure the accuracy of initial areal density in these films stays within 5%.

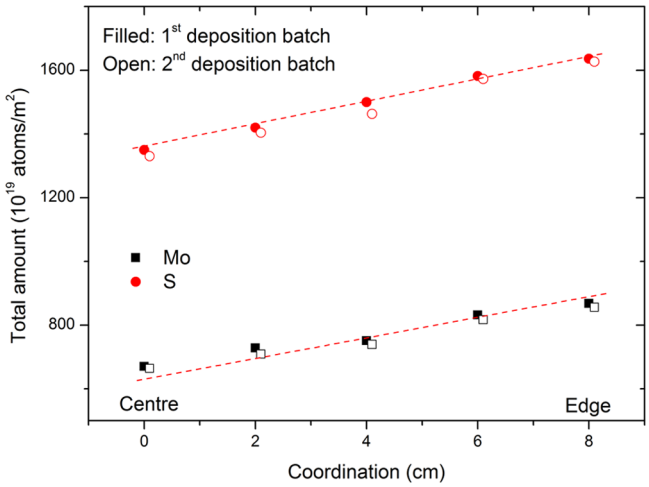

Figure 2. Total Mo and S areal density of MoS_2 films determined by RBS; the filled square and open circle symbol represent the samples deposited in two batches at different positions.

3.2. Compositional Changes. After deposition, MoS_2, Ti-doped MoS_2, and MoS_2/Ti multilayer films were exposed to the atomic oxygen with different incident fluence, and the corresponding composition changes were investigated by RBS. Figure 3a shows the 3 MeV ^{4}He RBS spectrum of as-deposited MoS_2 film and the MoS_2 films exposed to the atomic oxygen with incident fluence of 2.6×10^{19} O cm^{-2} and 1.2×10^{21} O cm^{-2}, respectively. After 2.6×10^{19} O cm^{-2} incident fluence exposure, the intensity of Mo peak remains the intensity as same as the initial sample, indicating no Mo atoms was removed during the exposure. Toward lower backscattering energy, an obvious feature in the spectrum is the decrease of the intensity of sulfur peak at the high energy edge, but at the low energy side the sulfur peak has the same intensity as the initial sample. Additionally, an oxygen signal on top of the silicon is observed at around 1100 keV. That means at lower fluence only the sulfur atoms located at near surface react with incident oxygen atoms. However, further increasing exposure fluence to 1.2×10^{21} O cm^{-2}, the intensity of sulfur peak throughout the whole backscattering region reduces by 40% compared to the initial sample, indicating the impinging atomic oxygen atoms not only react with the sulfur atoms at surface but also penetrate into depth and remove sulfur atoms at bottom. This is different when compared to the results reported

DOI: 10.1021/acsami.5b02709
ACS Appl. Mater. Interfaces 2015, 7, 12943−12950

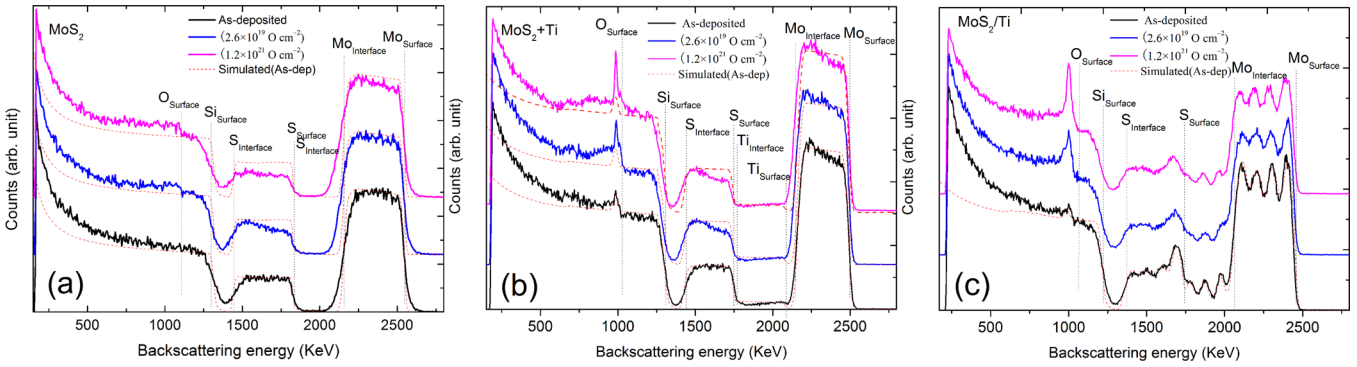

Figure 3. RBS spectra of (a) MoS_2, (b) Ti-doped, and (c) MoS_2/Ti multilayer films before and after atomic oxygen exposure to fluence of 2.6×10^{19} and 1.2×10^{21} O cm^{-2}, respectively. Except the backscattering energies of the surface and interface for Mo, S, and Si, the new emerge backscattering energy of O surface is marked by dotted line.

by Cross and Tagawa,[2,12] in which using XPS only a 3 nm thick oxidation layer was found at the surface of MoS_2 film after atomic oxygen exposure. It is also a surprise for us because the film's thickness is thicker than 1 μm, which is two or three orders of magnitude thicker than the penetration depth of the oxygen atom (about few nm), RBS data clearly revealed that this thick MoS_2 film does not block the transmission of atomic oxygen and the release of the erosion products. Although a small fraction of oxygen ions exists in atomic beam, but the flux of oxygen ion is 2 orders of magnitude lower comparing to atomic oxygen, furthermore, if we assume no energy loss during the incident beam impinging onto Mo plate, the energy of reflected oxygen ions equals to the floating potential, which should be below 20 eV, in this case the penetration depth of oxygen ions stays in few nm region. Clearly, the erosion depth is much deeper than the penetration depth of both oxygen atoms and ions, so we assume that a reaction pathway is present in the initial film, which allows the incident atomic oxygen to be able to reach the sulfur at bottom.

The RBS spectra of Ti-doped MoS_2 films before and after atomic oxygen exposure are shown in Figure 3b. Except the Mo, S, O, and Si peaks, the high-energy and low-energy edges of the Ti peak are marked as $Ti_{surface}$ and $Ti_{interface}$, respectively. From the data simulation, it can be known that titanium was doped homogeneously into MoS_2 films with 8% atomic concentration. Oxygen is also found in film with 10% atomic concentration and 20% atomic concentration at surface. The present of oxygen within the film can be attributed to the codeposition of impurity during sputtering process, in which the residual atmosphere in vacuum chamber could desorb and co-deposit with sputtered particles into the film. For higher oxygen concentration at the surface, results from the oxidation of titanium during long time air exposure. After 2.6×10^{19} O cm^{-2} incident fluence exposure, as same as we found in pure MoS_2 films, sulfur atoms are partially removed from the surface. However, further increasing incident fluence to 1.2×10^{21} O cm^{-2}, the sulfur peak at the low energy side has the same intensity as the initial sample, suggesting the sulfur atoms located at bottom are protected from further erosion. Furthermore, the intensity of higher oxygen concentration peak at the surface increases but not extends further to the low energy side, also proves that oxidation process happened only on the near surface.

For as-deposited MoS_2/Ti multilayer film, the Mo backscattering signal is interrupted by three dips which correspond to the three titanium interlayers between four MoS_2 layers. Although pure titanium interlayer deposited but the signal in each dip does not go to zero, that could be due to the atoms diffusion between Ti and MoS_2 interface. Unfortunately, the backscattering region of titanium and sulfur overlaps together so that the removal of sulfur due to the oxidation can not be directly seen from the spectra. But from the simulation results of SIMNRA we can get the integration of total sulfur amount in MoS_2/Ti multilayer, after atomic oxygen exposure to a fluence of 2.6×10^{19} O cm^{-2} about 7.8×10^{16} S cm^{-2} sulfur atoms is removed, and further increasing incident fluence to 2.6×10^{19} O cm^{-2}, the removed sulfur amount keeps as a constant that means the erosion process is suppressed or blocked.

Because the oxygen atom reacts with sulfur forming volatile SO_2 species, the main loss of MoS_2 film exposure to atomic oxygen source is the removing of sulfur atoms by incident atomic oxygen. Figure 4 summaries the removed sulfur amount

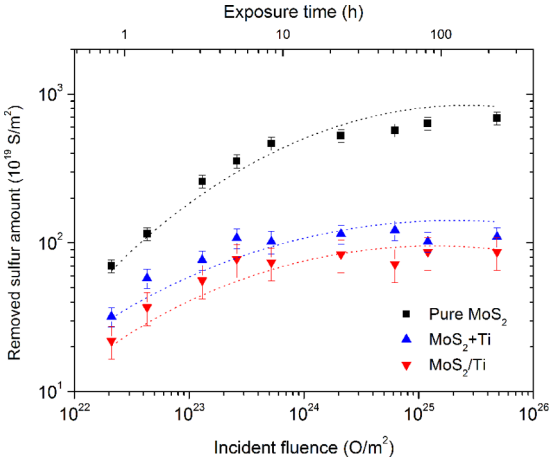

Figure 4. Removed sulfur amount of MoS_2, Ti-doped MoS_2, and MoS_2/Ti multilayer films exposed to the atomic oxygen as a function of the incident fluence. The dotted line is a guide to the eye.

of MoS_2 films determined by RBS and compared with Ti-doped MoS_2 and Ti/MoS_2 multilayer films as a function of incident fluence of atomic oxygen. Obviously, RBS results reveal that the erosion rate of Ti-doped MoS_2 and Ti/MoS_2 films is significantly lower than the rate of pure MoS_2 films, and it decreases with incident fluence. For the MoS_2 films, the removed sulfur amount increases with incident fluence, and turn to saturate at the end of our investigated fluence. At an incident fluence of 2.6×10^{19} O cm^{-2} (1 h atomic oxygen

DOI: 10.1021/acsami.5b02709
ACS Appl. Mater. Interfaces 2015, 7, 12943−12950

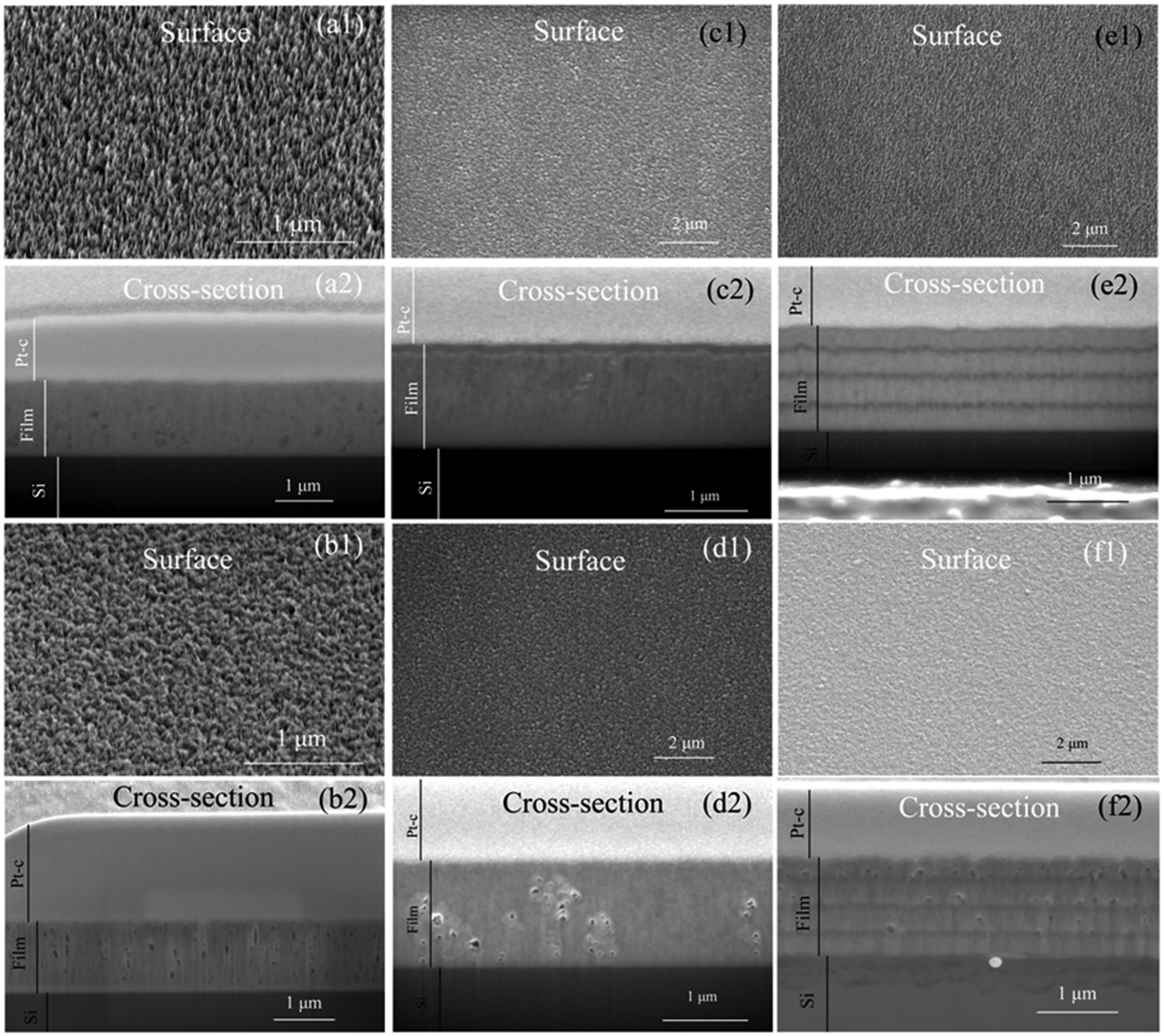

Figure 5. Surface and cross-section SEM images of as-deposited (a1, a2) MoS_2, (c1, c2) Ti-doped MoS_2, and (e1, e2) Ti/MoS_2 multilayer films, after atomic oxygen exposed (b1, b2) MoS_2, (d1, d2) Ti-doped MoS_2, and (f1, f2) Ti/MoS_2 multilayer films to a fluence of 2.1×10^{20} O cm^{-2}. The film and substrate and protecting Pt-c layer are marked by the lines. Note that the angle between the electron beam and the cross-section plane is 38° so that the vertical distances appear in the images shorter than they are in reality.

exposure) about 3.5×10^{17} S cm^{-2} sulfur was eroded, the corresponding erosion yield is 1.3×10^{-2}. Further increasing fluence to 6.2×10^{20} O cm^{-2} (24 h atomic oxygen exposure) the total removed sulfur amount increases to about 5.7×10^{17} S cm^{-2} and the corresponding erosion yield reduces by 2 orders of magnitude to 9.2×10^{-4}. Obviously, although incident oxygen atoms can penetrate into the depth of the film and erode the sulfur atoms at the bottom, but the diffusion of reactive oxygen species into depth is slow down with incident fluence, indicating the remaining films and newly formed oxidation partially block the diffusion of reactive oxygen species into depth. Compared to the pure MoS_2 film, doping titanium into MoS_2 reduces the sulfur removal rate significantly, the erosion yields of Ti-doped MoS_2 film at a fluence 2.6×10^{19} O cm^{-2} reduced by a factor of 3 from 1.3×10^{-2} to 4.1×10^{-3} compared to the pure MoS_2 film, and the removal sulfur amount tends to saturated at a fluence above 5.2×10^{19} O cm^{-2}. For Ti/MoS_2 films, the sulfur removal rate is even lower than Ti-doped MoS_2 film and tends to saturated after a fluence above 2.6×10^{19} O cm^{-2}, the removed sulfur amount at the corresponding fluence is 0.78×10^{17} S cm^{-2}, and the erosion yield is 3.0×10^{-3}.

3.3. Structural Changes. RBS results reveal clearly that doping 8% Ti or introducing Ti multilayer into MoS_2 films can reduce the erosion rate of sulfur and keep the film from the further erosion at certain fluence. To get more information about the structural evolution, MoS_2, Ti-doped MoS_2, and MoS_2/Ti multilayer films before and after the atomic oxygen exposure were investigated by FIB cross sectioning. Figure 5 shows the surface (a1) and cross-section (a2) images of MoS_2 film as-deposited and (b1, b2) after atomic oxygen exposure to a fluence of 2.1×10^{20} O cm^{-2}, respectively. The surface of as-deposited MoS2 films (Figure 5a1) shows an acicular and porous microstructure as same as reported in the literature,[21−23] after atomic exposure this acicular structure becomes more irregular (Figure 5b1). The total Mo and S

DOI: 10.1021/acsami.5b02709
ACS Appl. Mater. Interfaces 2015, 7, 12943−12950

atomic areal density of the identical film determined by RBS is 2.2×10^{18} Mo cm^2, this would correspond to a layer thickness of 1.22 μm if MoS_2 bulk density would be assumed, however, the actual thickness measured by cross-section image (Figure 5a2) is about 1.54 μm, indicating as-deposited MoS_2 film is not as dense as bulk, which is 21% lower than that of bulk density of MoS_2. The cross-section image also proves that pores with sizes from several tens nm up to nearly one hundred nm are irregularly distributed in the as-deposited film. According to RBS data evaluation, after atomic oxygen exposure although 40% sulfur atoms in the initial film were eroded by incident oxygen atoms; however, the thickness of the film remains largely unchanged (Figure 5b2), more pores with diameters ranging from tens to hundreds of nanometers appear, and these pores locate preferably along the direction perpendicular to the surface of substrate. As proved by RBS measurements, not only the sulfur atoms at the surface but also those from the bottom were eroded by incident oxygen atoms; because of its low impinging energy, we do not believe that atomic oxygen atom can penetrate a few hundred nanometers to react with sulfur in depth, so that we assume a reaction highway present in the film. It can be seen from Figure 5b that these newly formed pores preferably locate alone the direction perpendicular to the surface of substrate, which reveals that the erosion process happened mainly alone the boundaries of columnar grains. Because of the low density of as-deposited MoS_2 film, high density of cavity is present along the boundary of columnar structure, which allows the incident atomic oxygen to be able to reach the sulfur at bottom after a sufficiently high number of wall collisions within the film. Typically, doping Ti, Al, Au, etc. metal elements into transition metal dichalcogenides can increase the density of film and form nanocrystalline grains to strengthen the matrix and oxidation stability.[24−26] For Ti-doped MoS_2 films the surface image (Figure 5c1) shows a smooth, featureless and dense morphology, and from the corresponding cross-section image (Figure 5c2) the columnar structure is already not so obvious. The film thickness of Ti-doped MoS_2 film determined by the cross-section image is about 1.57 μm (Figure 5c2), and the corresponding total atomic areal density determined by RBS is 2.4×10^{18} Mo cm^2, based on these data a mass density of 4.1 g/cm^3 is achieved, which is still 15% lower than the density of bulk MoS_2 but higher than the density of as-deposited pure MoS_2 films. Although pore structures are still visible but the number density of cavity is much lower comparing to the as-deposited MoS_2 film. After atomic oxygen exposure no obvious change was found at surface (Figure 5d1) but more cavities appear within the film (Figure 5d2). Compared to the pure MoS_2 film, the distribution of pore structures in Ti-doped MoS_2 film is more irregular.

The surface of (Figure 5e1) MoS_2/Ti film shows the morphology as same as pure MoS_2 films, and these acicular and porous microstructures appear again. And multilayer structures are easily distinguished from the cross-section images of as-deposited MoS_2/Ti films in Figure 5e2. Unfortunately, the first titanium layer is invisible in the image due to its low contrast with silicon substrate. The three dark thin lines correspond to the titanium interlayer which separate four MoS_2 layers with the thickness about 320 nm. No defects such as pores or cracks were found in each MoS_2 layer of multilayer structure, it can be attributed to the multilayer structure that suppresses the growth of defects by introducing artificial interface. After atomic oxygen exposure (Figure 5f1), these acicular structures are almost invisible, again newly formed pore structures was found at the first top MoS_2 layer, which is similar as the situation of pure MoS_2 films exposure to the atomic oxygen. However, below the titanium interlayer, the number density of newly formed pore structures in the second MoS_2 layer decreases dramatically that means the present of titanium interlayer suppresses the erosion process happened below it. It is reported by Gouzman[27] that the atomic oxygen erosion of Kapton can be completely blocked by depositing 300 nm thick titania coating on it, but in our case, both RBS and SEM results confirmed that the erosion process still happened below the first Ti interlayer, it can be attributed to the thin thickness of Ti interlayer, obviously, 20 nm Ti interlayer is not thick enough to block the diffusion and reaction of impinging atomic oxygen with sulfur. The number density of formed cavity structures further decreases in third MoS_2 layers and completely disappears in the fourth MoS_2 layer, indicating the multilayer structure can eventually prevent the sulfur atoms from further erosion by incident atomic oxygen.

3.4. Tribological Properties. Because of the remarkable composition and structure changes of initial films resulted from the atomic oxygen exposure, speculations on the roles of sulfur substitution and oxygen erosion through the top surface to depth in determining the film tribological properties are also presented. Tribological tests were performed on a ball-on-disk tribometer in the low-pressure vacuum of 0.08 Pa, and AISI 400C steel balls with a diameter of 4 mm were used as counterparts with a normal load of 3 N and a ball sliding velocity of about 0.52 m/s. For example, Figure 6 plots the

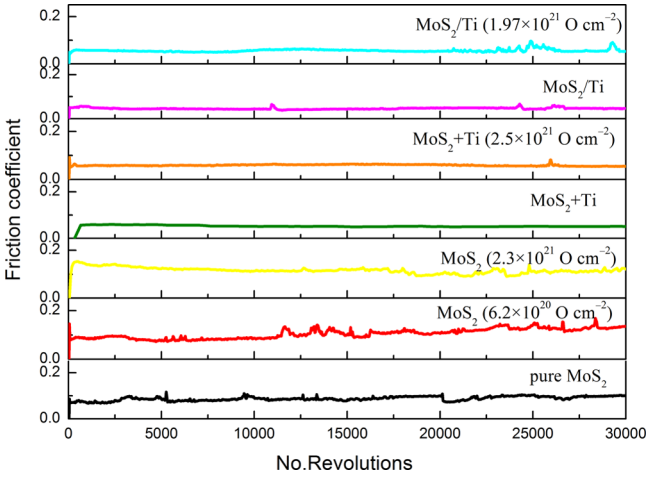

Figure 6. Friction coefficient curves of MoS_2, Ti-doped, and MoS_2/Ti multilayer films before and after atomic oxygen exposure for different incident fluence.

friction coefficient curves of MoS_2, Ti-doped and MoS_2/Ti multilayer films before and after atomic oxygen exposure for various exposure durations. For pure MoS_2 and its atomic oxygen irradiated films, a notable increase of friction coefficient approximately from 0.09 to 0.11 can be observed after a fluence 6.2×10^{20} O cm^{-2} (24 h atomic oxygen exposure), accompanied by a curve fluctuation after 10000 sliding revolutions, whereas a fluence 2.5×10^{21} O cm^{-2} (96 h atomic oxygen exposure) may lead to a further increase of friction coefficient above 0.14, along with a curve fluctuation starting from 20 000 sliding revolutions. Such a quick deterioration of lubrication is clearly attributed to the serious oxygen erosion on

DOI: 10.1021/acsami.5b02709
ACS Appl. Mater. Interfaces 2015, 7, 12943−12950

the top surface as well as the bottom through the grain boundaries and/or reaction pathway of columnar-structure and porous MoS_2 films as long as the exposure fluence exceeded 1.2 × 10^{21} O cm^{-2} (see in sec 3.2) in atomic oxygen exposure treatment. Correspondingly, the film wear rates of above-mentioned tribo-tests as described in Figure 7, added with the

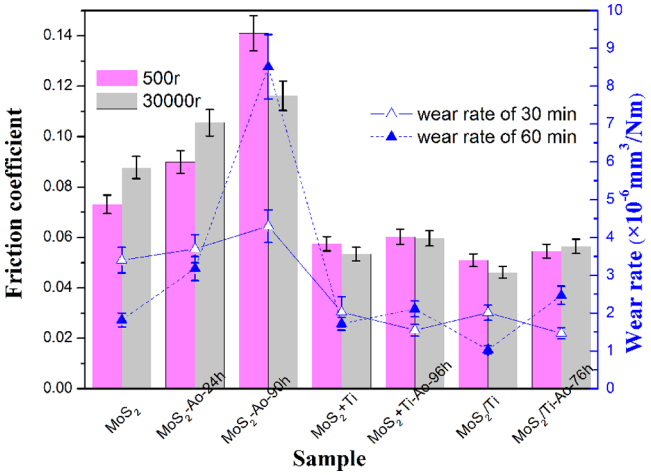

Figure 7. Mean friction coefficient of MoS_2, Ti-doped, and MoS_2/Ti multilayer films before and after atomic oxygen exposure for different exposure durations within 500r and 30000r tribo-tests.

mean friction coefficients derived from the beginning 500-revolution and long-time 30 000-revolution sliding tests indicate that for pure MoS_2 film and atomic oxygen irradiated films with a fluence of a fluence 6.2 × 10^{20} O cm^{-2} and 2.5 × 10^{21} O cm^{-2}, a liner increase in the mean friction coefficient occurs both in the beginning stage of sliding (approximately from 0.07 to 0.141) and the 30 000-revolution long-time sliding (approximately from 0.09 to 0.12); moreover, as the exposure fluence exceeded 6.2 × 10^{20} O cm^{-2}, a sharp jump of film wear rate from 3.18 × 10^{-6} mm^3/(N m) to 8.51 × 10^{-6} mm^3/(N m) is seen in long-time sliding tests. In comparison, a better situation can be seen in case of Ti-doped MoS_2 and its irradiated films at a fluence 2.5 × 10^{21} O cm^{-2} (96 h atomic oxygen exposure), which shows comparable initial friction coefficient of 0.055 and 0.06 respectively and then both slightly reduces in the following long-time sliding, producing relatively lower wear rate around 2 × 10^{-6} mm^3/N·m. It proves further that doping Ti into MoS_2 films can largely suppress the oxidation process merely occurring on the near-surface region and protect the MoS_2 lubricant phases from oxygen erosion at a certain extent, thereby exhibit better lubricant and antiwear properties. As expected, the lowest friction coefficient is achieved by the initial MoS_2/Ti multilayer film as 0.045, and stably kept as low as 0.052 after a 76 h atomic oxygen exposure treatment (a fluence 1.97 × 10^{21} O cm^{-2}). Thanks to the saturated sulfur removal rate after the fluence above 2.6 × 10^{19} O cm^{-2} (see in Sec.3.2), plus the well-confined erosion depth above the top Ti interlayer and the denser MoS_2 layer introduced by artificial interface, the intrinsic lubricant property of MoS_2 phase in vacuum sliding conditions is finely retained; accordingly, the mean friction coefficients of eroded MoS_2/Ti multilayer slightly increase from 0.052 to 0.054 and the wear rates are generally below 2.5 × 10^{-6} mm^3/(N m).

4. SUMMARY

In this work, MoS_2 and titanium-doped and MoS_2/Ti multilayer films were exposed to the atomic oxygen, and the erosion mechanism of these films was investigated as a function of incident fluence. The main erosion process of MoS_2 film exposure to the atomic oxygen source is the formation and releasing of volatile species by the reaction of oxygen with sulfur atoms. The erosion rate of pure MoS_2 films is significantly higher than the rate of titanium-doped and MoS_2/Ti multilayer films, although it decreases with increasing incident fluence but no saturation of erosion is detected in the investigated range. Surprisingly, RBS data indicates that the impinging atomic oxygen atoms not only react with the sulfur atoms at surface but also penetrate more than 1 μm into depth and remove sulfur atoms at bottom. More structural evolution details of these films before and after atomic oxygen exposure were investigated by FIB cross-section, the results reveal that high density of pores structures exists in the as-deposited MoS_2 films alone the boundary of columnar grain, which provides a reaction highway to the erosion process. The initial pore density decreases when titanium doping and MoS_2/Ti multilayer structures are introduced into films; consequently, the erosion highway is blocked and the erosion process is definitely suppressed. Further examination on the tribological properties of as-deposited and atomic oxygen irradiated films proves that revising MoS_2 lubricant films by doping Ti atoms or especially fabricating in MoS_2/Ti multilayer structure can effectively improve the film resistance to oxidation in atomic oxygen exposure, so that the instinct lubricant properties of MoS_2 phases can be well-retained in vacuum sliding conditions.

AUTHOR INFORMATION

Corresponding Author

*E-mail: pengwang@licp.cas.cn. Fax:+86-931-4968163. Tel: +86-931-4968236.

Author Contributions

The manuscript was written through contributions of all authors. All authors have given approval to the final version of the manuscript.

Notes

The authors declare no competing financial interest.

ACKNOWLEDGMENTS

The authors gratefully acknowledged the financial support from the National Natural Science Foundation of China (Grants 51227804, 11475236, and 91023041), 973 projects (2013CB632300) of the ministry of Science and Technology of China. Thanks are further due to Liang Gao (Max-Planck-Institut für Plasma-physik, Garching) for help with the RBS measurements.

REFERENCES

(1) Chambers, A. R.; Harris, I. L.; Roberts, G. T. Reactions of Spacecraft Materials with Fast Atomic Oxygen. *Mater. Lett.* **1996**, *26*, 121−131.

(2) Cross, J. B.; Martin, J. A.; Pope, L. E.; Koontz, S. L. Atomic Oxygen-MoS_2 Chemical Interactions. *Surf. Coat. Technol.* **1990**, *42*, 41−48.

(3) Pippin, H. G. Mechanisms of Atomic Oxygen Induced Materials Degradation. *Surf. Coat. Technol.* **1989**, *39/40*, 595−598.

(4) Woollam, J. A.; Synowicki, R. A.; Hale, J. S.; Ianno, N. J.; Blaine, L. Degradation of Thin Films: Comparison Between Low Earth Orbit

DOI: 10.1021/acsami.5b02709
ACS Appl. Mater. Interfaces 2015, 7, 12943−12950

Experiments and Laboratory Simulations of the Space Environment. *Thin Solid Films* **1994**, *241*, 218−221.
(5) Verker, R.; Grossman, E.; Eliaz, N. Erosion of POSS-polyimide Films under Hypervelocity Impact and Atomic Oxygen: The Role of Mechanical Properties at Elevated Temperatures. *Acta Materialia.* **2009**, *57*, 1112−1119.
(6) Grossman, E.; Gouzman, I. Space Environment Effects on Polymers in Low Earth Orbit. *Nucl. Instrum. Methods Phys. Res., Sect. B* **2003**, *208*, 48−57.
(7) Kiefer, R. L.; Anderson, R. A.; Kim, M. H. Y.; Thibeault, S. A. Modified Polymeric Materials for Durability in the Atomic Oxygen Space Environment. *Nucl. Instrum. Methods Phys. Res., Sect. B* **2003**, *208*, 300−302.
(8) Marciano, F. R.; Bonetti, L. F.; Pessoa, R. S.; Massi, M.; Santos, L. V.; Trava-Airoldi, V. J. Oxygen Plasma Etching of Silver-incorporated Diamond-like Carbon Films. *Thin Solid Films.* **2009**, *517*, 5739−5742.
(9) Gao, X.; Hu, M.; Sun, J.; Fu, Y.; Yang, J.; Weng, L. Changes in the Structure and Tribological Property of Ag Film by LEO Space Environment Exposure. *Appl. Surf. Sci.* **2014**, *320*, 466−470.
(10) Hu, M.; Gao, X.; Sun, J.; Weng, L.; Zhou, F.; Liu, W. The Effects of Nanoscaled Amorphous Si and SiN_x Protective Layers on the Atomic Oxygen Resistant and Tribological Properties of Ag Film. *Appl. Surf. Sci.* **2012**, *258*, 5683−5688.
(11) Ji, L.; Li, H.; Zhao, F.; Quan, W.; Chen, J.; Zhou, H. Atomic Oxygen Resistant Behaviors of Mo/diamond-like Carbon Nanocomposite Lubricating Films. *Appl. Surf. Sci.* **2009**, *255*, 4180−4184.
(12) Tagawa, M.; Yokota, K.; Matsumoto, K.; Suzuki, M.; Teraoka, Y.; Kitamura, A.; Belin, M.; Fontaine, J.; Martin, J. M. Space Environmental Effects on MoS_2 and Diamond-like Carbon Lubricating Films: Atomic Oxygen-induced Erosion and Its Effect on Tribological Properties. *Surf. Coat. Technol.* **2007**, *202*, 1003−1010.
(13) Gao, X.; Hu, M.; Sun, J.; Fu, Y.; Yang, J.; Liu, W.; Weng, L. Changes in the Composition, Structure and Friction Property of Sputtered MoS_2 Films by LEO Environment Exposure. *Appl. Surf. Sci.* **2015**, *330*, 30−38.
(14) Sui, X.; Gao, L.; Yin, P. Shielding Kevlar Fibers from Atomic Oxygen Erosion via Layer-by-layer Assembly of Nanocomposites. *Polym. Degrad. Stab.* **2014**, *110*, 23−26.
(15) Voevodin, A. A.; Zabinski, J. S. Nanocomposite and Nanostructured Tribological Materials for Space Applications. *Compos. Sci. Technol.* **2005**, *65*, 741−748.
(16) Baker, C. C.; Hu, J. J.; Voevodin, A. A. Preparation of Al_2O_3/DLC/Au/MoS_2 Chameleon Coatings for Space and Ambient Environments. *Surf. Coat. Technol.* **2006**, *201*, 4224−4229.
(17) Baker, C. C.; Chromik, R. R.; Wahl, K. J.; Hu, J. J.; Voevodin, A. A. Preparation of Chameleon Coatings for Space and Ambient Environments. *Thin Solid Films* **2007**, *515*, 6737−6743.
(18) Hechtl, E.; Eckstein, W.; Roth, J.; Laszlo, J. Sputtering of Tungsten by Oxygen at Temperatures up to 1900 K. *J. Nucl. Mater.* **1991**, *179*, 290−293.
(19) Mayer, M. Codeposition of Deuterium with BeO at Elevated Temperatures. *J. Nucl. Mater.* **1997**, *240*, 164−167.
(20) Wang, P.; Jacob, W.; Gao, L.; Dürbeck, T.; Schwarz-Selinger, T. Comparing Deuterium Retention in Tungsten Films Measured by Temperature Programmed Desorption and Nuclear Reaction Analysis. *Nucl. Instrum. Methods Phys. Res., Sect. B* **2013**, *300*, 54−61.
(21) Hwang, M. J.; Kim, K. M.; Ryu, K. S. Effects of Graphene on MoO_2-MoS_2 Composite as Anode Material for Lithium-ion Batteries. *J. Electroceram.* **2014**, *33*, 239−245.
(22) Deepthi, B.; Barshilia, H. C. Nanostructured Solid Lubricant Coatings for Aerospace Applications. *Aerosp. Mater. Handb.* **2012**, 359.
(23) Hilton, M. R.; Fleischauer, P. D. TEM Lattice Imaging of the Nanostructure of Early-growth Sputter-deposited MoS_2 Solid Lubricant Films. *J. Mater. Res.* **1990**, *5*, 406−421.
(24) Lince, J. R.; Hilton, M. R.; Bommannavar, A. S. EXAFS of Sputter-deposited MoS_2 Films. *Thin Solid Films* **1995**, *264*, 120−134.
(25) Nainaparampil, J. J.; Phani, A. R.; Krzanowski, J. E.; Zabinski, J. S. Pulsed Laser-ablated MoS_2-Al Films: Friction and Wear in Humid Conditions. *Surf. Coat. Technol.* **2004**, *187*, 326−335.
(26) Teer, D. G. New Solid Lubricant Coatings. *Wear.* **2001**, *251*, 1068−1074.
(27) Gouzman, I.; Girshevitz, O.; Grossman, E.; Eliaz, N.; Sukenik, C. N. Thin Film Oxide Barrier Layers: Protection of Kapton from Space Environment by Liquid Phase Deposition of Titanium Oxide. *ACS Appl. Mater. Interfaces* **2010**, *2*, 1835−1843.

DOI: 10.1021/acsami.5b02709
ACS Appl. Mater. Interfaces 2015, 7, 12943−12950